

Feedback Control Goes Wireless: Guaranteed Stability over Low-power Multi-hop Networks

Fabian Mager*
TU Dresden

Dominik Baumann*
MPI for Intelligent Systems

Romain Jacob
ETH Zurich

Lothar Thiele
ETH Zurich

Sebastian Trimpe
MPI for Intelligent Systems

Marco Zimmerling
TU Dresden

ABSTRACT

Closing feedback loops fast and over long distances is key to emerging applications; for example, robot motion control and swarm coordination require update intervals below 100 ms. Low-power wireless is preferred for its flexibility, low cost, and small form factor, especially if the devices support multi-hop communication. Thus far, however, closed-loop control over multi-hop low-power wireless has only been demonstrated for update intervals on the order of multiple seconds. This paper presents a wireless embedded system that tames imperfections impairing control performance such as jitter or packet loss, and a control design that exploits the essential properties of this system to provably guarantee closed-loop stability for linear dynamic systems. Using experiments on a testbed with multiple cart-pole systems, we are the first to demonstrate the feasibility and to assess the performance of closed-loop control and coordination over multi-hop low-power wireless for update intervals from 20 ms to 50 ms.

1 INTRODUCTION

Cyber-physical systems (CPS) use embedded computers and networks to monitor and control physical systems [21]. While monitoring using *sensors* allows, for example, to better understand environmental processes [18], it is control through *actuators* what nurtures the visions of robotic materials [19], intelligent transportation [2], smart buildings [20], or automated medical treatment [68]. A key problem, however, is how to close the *feedback loops* between sensors and actuators as they may be numerous, mobile, distributed across large spaces, and attached to devices with size, weight, and cost constraints. This is particularly challenging for physical systems with fast dynamics, as feedback must be significantly faster than the physical systems evolve [5]. Moreover, because feedback modifies the dynamics of physical systems, guaranteeing *closed-loop stability* is a major concern [6].

In this paper, we ask the following question: *Can we enable fast closed-loop control over multi-hop low-power wireless networks with provable guarantees on stability?* Since three

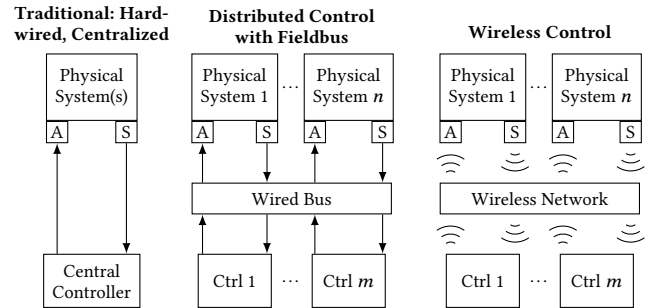


Figure 1: Evolution of control architectures. *Physical systems with sensors (S) and actuators (A) are connected to controllers (Ctrl) over point-to-point wires (left), a wired bus (center), or a wireless network (right).*

decades there has been a strong push towards wireless technology in industrial settings, as it reduces installation and maintenance costs dramatically [43]. On top of that, low-power solutions and multi-hop communication offer the flexibility and mobility required to realize the CPS vision [75]. Consequently, industrial consortia are actively driving standardization efforts to further promote low-power wireless for industrial communications and beyond [72].

Challenges. Despite clear advantages and the anticipated next major breakthrough in distributed automation and control, closing feedback loops over wireless poses significant challenges for control design [7, 34, 50, 78]. These are rooted in the architectures that have traditionally been considered.

In traditional control systems, sensors and actuators are connected to a *centralized* controller via point-to-point wires (Fig. 1, left) [7]. Although centralized control is beneficial because the controller has all information, it is often impractical for large-scale systems. An alternative is *decentralized* control, where the system is split into a number of subsystems, each connected to a local controller, but without signal transfer between them [50, 78]. However, decentralized control can exhibit poor performance and it may not even be possible to achieve closed-loop stability [78]. Hence, communication networks in the form of *wired busses* were introduced [7] (Fig. 1, center), which are still widely used in automation and

*Both authors contributed equally to this work.

control today [71, 73]. Replacing a wired bus with a wireless network (Fig. 1, right) presents five main challenges:

- *Limited bandwidth.* Wireless networks have more severe constraints on the amount of information that can be transferred per unit of time. Because feedback control requires timely transfer of information (e.g., to stabilize unstable processes [74]), this is critical. Owing to limited bandwidth, there is also a trade-off between the number of supported sensors and actuators and the *update interval*, the interval with which sensor values can be acquired and actuation commands can be applied.
- *Delay and jitter.* While in wired point-to-point connections communication delays are typically small enough to be neglected, they cannot be ignored in a wireless network. What is more, network delays are subject to random variations, introducing significant jitter. Delays and jitter can both destabilize a feedback system [76].
- *Message loss.* Wireless communication is orders of magnitude less reliable than wired communication. Because corrupt or lost messages disrupt feedback, they complicate control design. Moreover, as message losses often occur in bursts [67], a valid theoretical analysis to provide strong guarantees is challenging, if not impossible.
- *Constrained traffic pattern.* Wired busses inherently support many-to-all communication and hence centralized control. Coordination between control computations by different devices is straightforward, allowing for a common control objective (e.g., platooning [9]), dynamic couplings between physical systems (e.g., process control [83]), and cooperative resource sharing (e.g., traffic management [45]). Wireless multi-hop networks typically support only distinct traffic patterns, such as 1-hop broadcast, many-to-one collection, or one-to-all dissemination. Control under constrained traffic patterns is more challenging and may imply poor performance or even infeasibility of closed-loop stability [78].
- *Message duplicates and out-of-order arrivals.* Finally, message duplicates and out-of-order message arrivals are typical in wireless protocols [22, 30], but further hinder control design and stability analysis [81].

Practical efforts to tackle these challenges fall in two categories. First, multi-hop low-power wireless solutions exist for physical systems with slow dynamics achieving update intervals of tens of seconds, albeit without stability guarantees [12, 59]. Second, wireless solutions for faster dynamics providing updates every tens of milliseconds have also been demonstrated, but only in single-hop settings [8, 23, 52, 55, 79]. This leaves a significant gap to the many CPS applications that would be enabled or benefit from fast closed-loop control and coordination with stability guarantees over multi-hop low-power wireless networks [1, 32, 51].

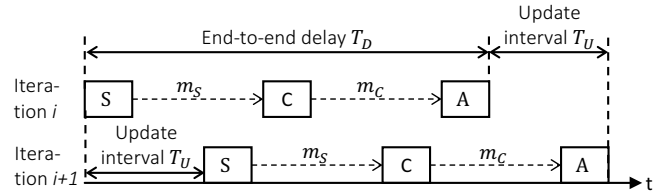


Figure 2: Execution of application tasks and message transfers over time for a single periodic feedback loop. In every iteration, the sensing task (S) takes a measurement of the physical system and sends it to the control task (C). The control task computes a control signal and sends it to the actuation task (A), which applies it on the physical system.

Contributions. This paper presents the first design, analysis, and evaluation of a system that closes this gap. To address the challenges outlined above, we co-design the wireless embedded elements along with the control system. Specifically, we tame imperfections such as delay, jitter, and message losses through a novel end-to-end design of the embedded computing and wireless communication components. Then, we consider the essential properties of the wireless embedded system in the control design, targeting the many practical systems whose dynamics can be faithfully approximated by a linear model [6, 35]. Through a formal analysis, we guarantee closed-loop stability for the wireless control system.

To validate and evaluate our approach, we implement the overall design on a testbed of state-of-the-art low-power wireless devices forming a 3-hop network. The testbed includes multiple cart-pole systems, whose temporal dynamics match a range of real-world mechanical systems and is hence extensively used for research in control [6, 73]. Our experiments reveal the following key findings: (i) two inverted pendulums can be safely stabilized via a remote controller across the 3-hop network; (ii) the movement of three cart-poles can be synchronized reliably over the network; (iii) increasing packet loss rates and update intervals can be tolerated, but deteriorate the control performance; and (iv) key assumptions made in the theoretical derivations are valid.

2 OVERVIEW

System architecture. According to Fig. 1, we consider distributed CPS where the *application tasks* of sensing, actuation, and control are mapped onto a set of low-power embedded devices with the required hardware capabilities. A device may execute multiple application tasks, which may belong to different periodic feedback loops. All devices have a low-power wireless radio and are capable of multi-hop communication. Using this capability, the application tasks exchange *messages* with each other to close the control loops.

Fig. 2 shows the execution of application tasks and the exchange of messages over time for a single periodic feedback

loop with one sensor and one actuator. The *update interval* T_U is the time between the start (resp. end) of consecutive sensing (resp. actuation) tasks. The *end-to-end delay* T_D is the time between the start of a sensing task until the end of the actuation task that applies the corresponding control signal on the physical system.

Design goals. We adopt the following co-design approach: *Address the challenges from above on the wireless embedded system side to the extent possible, then take into account the resulting key properties in the control design.* This entails the design of a wireless embedded system that aims to

- G1** eliminate or, if this is impossible, reduce and bound imperfections impairing control performance (e.g., reduce T_U and T_D and bound the jitter on these);
- G2** support arbitrary traffic patterns in the face of dynamically changing network topologies;
- G3** operate efficiently in terms of energy, while accommodating the computational needs of the controller.

In turn, the control design, which determines the functionality of the application tasks, aims to

- G4** incorporate all essential properties of the wireless embedded system to guarantee closed-loop stability for the entire CPS with linear dynamics;
- G5** enable an efficient implementation of the control logic on state-of-the-art low-power embedded devices;
- G6** exploit support for arbitrary traffic patterns for straightforward implementation of distributed control.

Outline. In the following, §3 details the design and implementation of the wireless embedded system components, while §4 focuses on the control design and stability analysis.

3 DESIGN AND IMPLEMENTATION OF WIRELESS EMBEDDED SYSTEM

Our solution to reach goals **G1–G3** is an embedded system design that consists of three building blocks:

- 1) a *low-power wireless protocol* providing multi-hop many-to-all communication with bounded delay and accurate network-wide time synchronization;
- 2) an *embedded hardware architecture* that enables an efficient and timing-predictable execution of all application tasks and message transfers;
- 3) a *scheduling framework* that globally schedules all application tasks and message transfers such that application-specific bounds on T_U and T_D are met at minimum energy costs for wireless communication.

We describe each building block, followed by an analysis of the resulting properties that matter for control design.

3.1 Low-power Wireless Protocol

To support arbitrary traffic patterns (**G2**), we require a multi-hop protocol that is capable of many-to-all communication

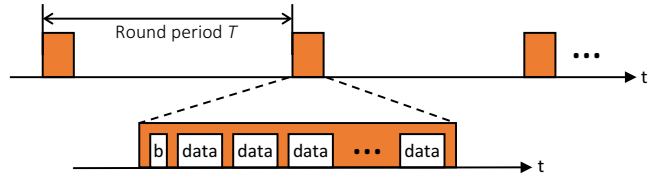


Figure 3: Time-triggered operation of multi-hop low-power wireless protocol. Communication occurs in rounds with a given round period T . Every beacon (b) and data slot in a communication round is a network-wide Glossy flood.

from any set of source nodes. Moreover, the protocol must be highly reliable and the time needed for many-to-all communication should be tightly bounded, if not deterministic (**G1**). It has been shown that a solution based on network-wide Glossy floods [26] can meet these requirements with high efficiency (**G3**) and resilience to network dynamics (**G2**) [85]. Therefore, similar to other recent proposals [25, 36], we design a wireless protocol on top of Glossy, but target a unique design point: bounded latencies of a few tens of milliseconds for many-to-all communication.

As shown in Fig. 3, the operation of our protocol proceeds as a series of periodic *communication rounds* with *period* T . Each round consists of a sequence of time *slots*. In each time slot, all nodes in the network participate in a Glossy flood, where a message is disseminated from an initiator to all other nodes. Glossy achieves the theoretical minimum latency for one-to-all flooding at a reliability above 99.9%, operates independently of the time-varying network topology, and provides microsecond-level network-wide time synchronization [26]. Nodes leverage the time synchronization to sleep between communication rounds and to awake in time for the next round as specified by the round period T .

Every round begins with a *beacon slot*, wherein a dedicated node, called *host*, sends a small packet. Then, up to B *data slots* follow. In each data slot, one node is allowed to transmit a message to all other nodes by initiating a Glossy flood.

As detailed in §3.3, we compute the communication schedules offline based on the application’s traffic demands, and distribute them to all nodes before the application operation starts. A communication schedule includes the assignment of messages/initiators to data slots in a round and the round period T . The beacon sent by the host at the beginning of a round contains the current schedule index. Using this index, nodes look up the schedule for the current round.

Using static communication schedules has several benefits. First, it matches the requirements of mission- or safety-critical CPS applications, which regard runtime adaptability as a potential source of failure [40, 57]. Second, we support significantly shorter latencies compared to prior work [25, 36, 85]. Third, we can a priori verify if closed-loop stability can be guaranteed for the achievable latencies (see §4). Fourth,

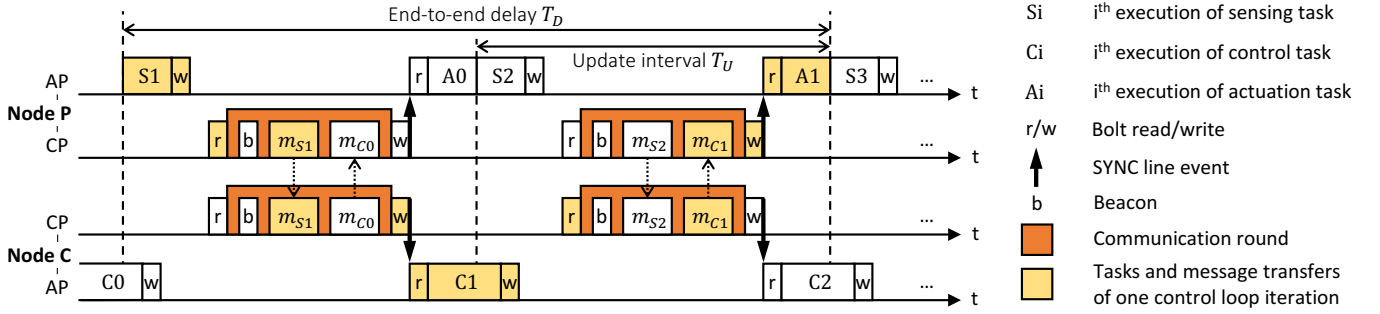


Figure 4: Example schedule of tasks and message transfers between two dual-processor platforms. *Node P senses and acts on a physical system; C runs the controller. In the current design, the update interval T_U is half the end-to-end delay T_D .*

the protocol is more resilient to packet loss (particularly lost beacons), thus improving reliability and energy efficiency.

3.2 Embedded Hardware Architecture

CPS devices need to concurrently handle application tasks and message transfers. While message transfers involve little, but frequent computation (e.g., inside interrupt service routines), sensing and especially control tasks require less frequent but more demanding computations (e.g., matrix and floating-point operations). An effective approach to achieve low latency and high energy efficiency for such diverse needs is to exploit hardware heterogeneity.

For this reason, we leverage a heterogeneous *dual-processor platform (DPP)*. Application tasks execute exclusively on a 32-bit MSP432P401R ARM Cortex-M4F *application processor* (AP) running at 48 MHz, while the wireless protocol executes on a dedicated 16-bit CC430F5147 *communication processor* (CP) running at 13 MHz. The AP features a floating-point unit and a rich instruction set, accelerating operations related to sensing and control. The CP integrates a microcontroller and a low-power wireless radio operating at 250 kbit/s in the 868 MHz band with 2-GFSK modulation on a single chip.

AP and CP are interconnected using Bolt [70], an ultra-low-power processor interconnect that supports asynchronous bi-directional message passing with formally verified worst-case execution times. Bolt decouples the two processors with respect to time, power, and clock domains, enabling energy-efficient concurrent executions with only small and bounded interference, thereby limiting jitter and preserving the time-sensitive operation of the wireless protocol.

Nevertheless, we require AP and CP to share a common time base to reduce end-to-end delays between application tasks running on different APs. To this end, we use a GPIO line between the two processors, called the *SYNC* line. Every CP asserts the SYNC line in response to an update of Glossy’s network-wide time synchronization. Every AP schedules application tasks and message passing over Bolt with specific offsets relative to these SYNC line events. Likewise, the CPs

execute the communication schedules and schedule SYNC line assertion and message passing over Bolt with specific offsets relative to the start of communication rounds. As a result, all APs and CPs act in concert. Next, we describe how we compute the communication schedules and offsets.

3.3 Scheduling Framework

We first illustrate the scheduling problem with a simple example. In CPS physical process (P) and control (C) are, in general, distributed across different nodes; here we consider two nodes as an example: Node P senses and acts on a physical system, and node C runs the controller.

Fig. 4 shows a possible schedule of the application tasks and message transfers. After sensing (S₁), the AP of P writes a message containing the sensor reading into Bolt (w). CP reads out the message (r) before the communication round in which that message (m_{S₁}) is sent using the wireless protocol. The CP of node C receives the message and writes it into Bolt. After reading out the message from Bolt, AP computes the control signal (C₁) and writes a message containing it into Bolt. The message (m_{C₁}) is sent to node P in the next communication round, whose AP applies the control signal on the physical system (A₁).

This schedule yields a kind of pipelined execution, where in each communication round the last sensor reading and the next control signal (computed based on the previous sensor reading) are exchanged (m_{S₁} m_{C₀}, m_{S₂} m_{C₁}, . . .). Note that while it is indeed possible to send the corresponding control signal in the same round (m_{S₁} m_{C₁}, . . .), this would increase the update interval T_U at least by the sum of the execution times of the control task, Bolt read, and Bolt write. For the schedule in Fig. 4, T_U is exactly half the end-to-end delay T_D .

In general, the scheduling problem entails computing the communication schedules (i.e., assignment of messages to slots in each round and period T) and the offsets with which APs (relative to SYNC line events) and CPs (relative to start of communication rounds) perform wireless communication, application tasks, message transfers over Bolt, or SYNC

line assertion. The problem gets extremely complex for any realistic scenario with more nodes and possibly multiple concurrent control loops, so solving it should be automated.

To this end, we use Time-Triggered Wireless (TTW) [37], an existing framework that requires only minimal changes to solve the above scheduling problem. TTW takes as main input a dependency graph among application tasks and messages, similar to Fig. 2. Based on an integer linear program, it computes all communication schedules and offsets (see [37] for a detailed description of the inputs). TTW provides three important guarantees: (i) a feasible solution is found if one exists, (ii) the solution has the minimum number of communication rounds and thus minimizes communication energy consumption within the constraints of the wireless protocol, and (iii) the solution can optimize user-defined metrics, such as the update interval T_U as for the schedule in Fig. 4.

3.4 Essential Properties

The presented wireless embedded system provides the following key properties for the control design:

- P1** As analyzed below, for update intervals T_U and end-to-end delays T_D up to 100 ms, the worst-case jitter on T_U and T_D is a few tens of microseconds. It holds $T_D = 2T_U$.
- P2** Statistical analysis of millions of Glossy floods [84] and percolation theory for time-varying networks [39] have shown that the spatio-temporal diversity in a flood reduces the temporal correlation in the series of received and lost messages by a node, to the extent that the series can be safely approximated by an i.i.d. Bernoulli process. The success probability is typically above 99.9% [26].
- P3** By provisioning for multi-hop many-to-all communication, arbitrary traffic patterns are supported.
- P4** It is guaranteed by design that message duplication and out-of-order message delivery cannot occur.

The combination of **P1–P4** in an end-to-end low-power wireless system is indeed unique. Previous work on control over low-power wireless [4, 8, 12, 62] reports jitter larger than tens of milliseconds, must deal with highly correlated messages losses over individual links [66], is limited to either single-hop networks or constrained traffic patterns, and exposed to message duplicates and out-of-order arrivals.

Jitter analysis. We are interested in the *worst-case* jitter on T_U and T_D . To this end, we look at the time interval between the *end* of two periodic tasks running on *different* APs. The nominal length of the interval is \tilde{T}_{end} , but due to jitter J its length is $\tilde{T}_{end} + J$. In our system, the jitter is bounded by

$$|J| \leq 2(\hat{e}_{ref} + \hat{e}_{SYNC} + \tilde{T}_{end}(\hat{\rho}_{AP} + \hat{\rho}_{CP})) + \hat{e}_{task}. \quad (1)$$

Below, we detail the different sources of jitter affecting (1).

1) *Time synchronization error between CPs.* Using Glossy, each CP computes an estimate \hat{t}_{ref} of the reference time [26],

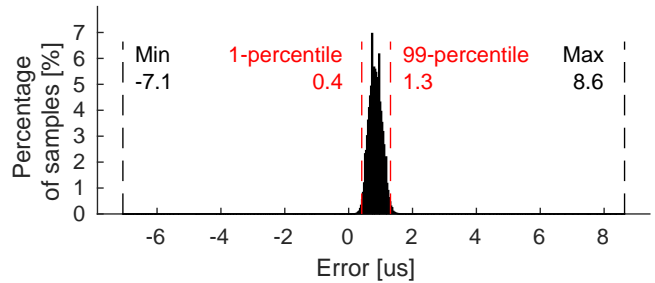


Figure 5: Synchronization error of our Glossy implementation for a network diameter of up to nine hops. The error is typically below 1.5 μs . The long tail on both sides is due to a race condition in an interrupt service routine.

which it uses to schedule subsequent activities. In doing so, each CP makes an error e_{ref} with respect to the reference time of the initiator. Using the approach from [26], we measure e_{ref} for our Glossy implementation and a network diameter of up to 9 hops. We can see from Fig. 5 that e_{ref} is typically less than 1.5 μs ; the long tail on both sides is due to a race condition in an interrupt service routine. Nevertheless, based on 340,000 data points, e_{ref} is always between -7.1 μs and 8.6 μs . We thus consider $\hat{e}_{ref} = 10 \mu\text{s}$ to be a safe bound for the jitter on the reference time across CPs.

2) *CP and AP sourced by independent clocks.* Each AP schedules activities relative to SYNC line events. As AP and CP are sourced by independent clocks, it takes a variable amount of time until AP detects that CP asserted the SYNC line. The resulting jitter is bounded by $\hat{e}_{SYNC} = (2f_{AP})^{-1}$, where $f_{AP} = 48 \text{ MHz}$ is the frequency of AP’s clock in our system.

3) *Different clock drift at CPs and APs.* The real offsets and durations of activities on the CPs and APs depend on the frequency of their clocks. Various factors such as manufacturing process, temperature, and aging lead to different frequency drifts ρ_{CP} and ρ_{AP} of the clocks. State-of-the-art clocks, however, drift by at most $\hat{\rho}_{CP} = \hat{\rho}_{AP} = 50 \text{ ppm}$ [42].

4) *Varying task execution times.* The difference between the task’s best- and worst-case execution time \hat{e}_{task} adds to the jitter. For the jitter on T_U and T_D , only the execution time of the actuation task matters, which typically exhibits little variance as it is short and highly deterministic. For example, actuation in our experiments in §5.2 has a jitter of $\pm 3.4 \mu\text{s}$. To be safe, we consider $\hat{e}_{task} = 10 \mu\text{s}$ for our analysis.

Using (1) and the above values, we can compute the worst-case jitter for a given interval \tilde{T}_{end} . Fast closed-loop control as considered in this paper requires $\tilde{T}_{end} = T_D = 2T_U \leq 100 \text{ ms}$, which gives a worst-case jitter of $\pm 50 \mu\text{s}$, as stated in **P1**.

4 CONTROL DESIGN AND ANALYSIS

Building on the design of the wireless embedded system and properties **P1–P4**, this section addresses the design of the

control system to accomplish goals **G4–G6** from §2. Because the wireless system supports arbitrary traffic patterns (**P3**), various control tasks can be solved including typical single-loop tasks such as stabilization, disturbance rejection, or set-point tracking, as well as multi-agent scenarios such as synchronization, consensus, or formation control.

Here, we focus on remote stabilization over wireless and synchronization of multiple agents as prototypical examples for both the single- and multi-agent case. For stabilization, we detail our approach for modeling, control design, and stability analysis in §4.1 to §4.3, thus achieving **G4–G5**. Synchronization is discussed in §4.4, highlighting support for straightforward distributed control according to **G6**.

4.1 Model of Wireless Control System

We address the remote stabilization task depicted in Fig. 6 (left), where controller and physical process are associated with different nodes, which are connected by the wireless system of §3. As the physical process, we consider linear time-invariant (LTI) dynamics. LTI models capture the dynamics of many practical systems in their operating range sufficiently well and are the predominant model in control engineering [6, 35]. The (stochastic) LTI state-space model

$$x(k+1) = Ax(k) + Bu(k) + v(k) \quad (2a)$$

describes the evolution of the system state $x(k) \in \mathbb{R}^n$ with discrete time index $k \in \mathbb{N}$ in response to control input $u(k) \in \mathbb{R}^m$ and random process noise $v(k) \in \mathbb{R}^n$. The process noise is modeled as an independent identically distributed (i.i.d.) Gaussian random variable with zero mean and variance Σ_{proc} ($v(k) \sim \mathcal{N}(0, \Sigma_{\text{proc}})$) and captures uncertainty in the model. Model parameters (in particular matrices A and B) are typically obtained from first principles or system identification [6]. The transition matrix A is essential for the stability properties of the system: The system (2a) is unstable (i.e., the state $x(k)$ diverges for $k \rightarrow \infty$) if, and only if, A has an eigenvalue with magnitude greater than one [35].

We assume that the full system state $x(k)$ can be measured through appropriate sensors, that is,

$$y(k) = x(k) + w(k) \quad (2b)$$

with sensor measurements $y(k) \in \mathbb{R}^n$ and sensor noise $w(k) \in \mathbb{R}^n$, $w(k) \sim \mathcal{N}(0, \Sigma_{\text{meas}})$. If the complete state vector cannot be measured directly, it can typically be reconstructed via state estimation techniques [35].

The process model (2) is stated in discrete time; that is, the discrete-time signal $s(k)$ represents the sample of the continuous-time signal $s(t)$ at time $t = kT_s$, where T_s is the sampling time. This representation is particularly suitable here as the wireless system offers a nearly constant update time T_U with jitter in the order of tens of μs (**P1**), which can be neglected from controls perspective [14, 65]. Thus, we set

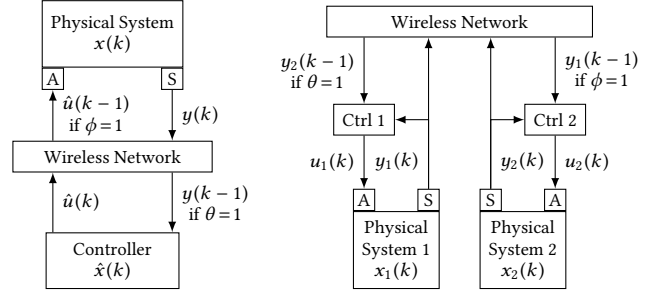


Figure 6: Considered wireless control tasks: stabilization (left) and synchronization (right). On the left, the feedback loop for stabilizing the physical system is closed over the (multi-hop) low-power wireless network, which induces delay and packet losses (captured by i.i.d. Bernoulli variables θ and ϕ). On the right, two physical systems, each with a local controller (Ctrl), are synchronized over the wireless network.

$T_s = T_U$, and $u(k)$ and $y(k)$ in (2) then represent sensing and actuation at periodic intervals T_U as in Fig. 4.

As shown in Fig. 6, measurements $y(k)$ and control inputs $\hat{u}(k)$ are sent over the wireless network. According to **P1** and **P2**, both arrive at the controller resp. system with a delay of T_U and with a probability governed by two independent Bernoulli processes. We represent the Bernoulli processes by $\theta(k)$ and $\phi(k)$, which are i.i.d. binary variables, indicating lost ($\theta(k) = 0$ resp. $\phi(k) = 0$) or successfully received packets ($\theta(k) = 1$ resp. $\phi(k) = 1$). To ease notation and since both variables are i.i.d., we can omit the time index in the following without any confusion. We denote the probability of successful delivery by μ_θ (i.e., $\mathbb{P}[\theta = 1] = \mu_\theta$) resp. μ_ϕ . As both, measurements and control inputs, are delayed, it also follows that in case of no packet loss, the applied control input $u(k)$ depends on the measurement two steps ago $y(k-2)$. In case a control input packet is lost, the input stays constant because zero-order hold is used at the actuator; hence

$$u(k) = \phi \hat{u}(k-1) + (1-\phi)u(k-1). \quad (3)$$

The model proposed in this section thus captures the properties **P1**, **P2**, and **P4**. While **P1** and **P2** are incorporated in the presented dynamics and packet loss models, **P4** means that there is no need to take duplicated or out-of-order sensor measurements and control inputs into account. Overall, these properties allow for accurately describing the wireless CPS by a fairly straightforward model, which will greatly facilitate subsequent control design and analysis. Property **P3** is not considered here, where we deal with a single control loop, and will become relevant only in §4.4.

4.2 Controller Design

We design a feedback controller for the system in (2), which maps measurements $y(k)$ to control inputs $u(k)$. Through

feedback, we can modify the state dynamics (2a) and, for example, stabilize an otherwise unstable system (as done in the experiments in §5). Feedback control can also be helpful for stable A to obtain desirable dynamics properties (e.g., fast response or damping). We proceed by first discussing state-feedback control for the nominal system (i.e., without delays, packet losses, and noise), and then enhance the design to cope with non-ideal measurements and communication.

Nominal design. Assuming ideal measurements, we have $y(k) = x(k)$. A common control strategy in this setting is static state-feedback control, $u(k) = Fx(k)$, where F is the constant feedback matrix to be designed. Inserting this controller in (2a) yields $x(k+1) = (A + BF)x(k) + v(k)$. That is, we can modify the transition matrix through state feedback ($A + BF$ instead of A) and thus modify the state dynamics. Under the assumption of controllability [35], we can place all eigenvalues of $A + BF$ to desired locations and, in particular, choose them to have magnitude less than one resulting in stable closed-loop dynamics. In classical control theory [3, 6, 35], there are various methods to design such an F , for example, *pole placement* or optimal control such as the *linear quadratic regulator* (LQR).

Actual design. We augment the nominal state-feedback design to cope with non-idealities, in particular, delayed measurements and packet losses as shown in Fig. 6 (left).

Because the measurement arriving at the controller $y(k-1)$ represents information that is one time step in the past, the controller propagates the system for one step as follows:

$$\begin{aligned}\hat{x}(k) &= \theta Ay(k-1) + (1-\theta)(A\hat{x}(k-1)) + B\hat{u}(k-1) \\ &= \theta Ax(k-1) + (1-\theta)A\hat{x}(k-1) + B\hat{u}(k-1) + \theta Aw(k-1),\end{aligned}\quad (4)$$

where $\hat{x}(k)$ is the predicted state, and $\hat{u}(k)$ is the control input computed by the controller (to be made precise below). Both variables are computed by the controller and represent its internal states. The rationale of (4) is as follows: If the measurement packet is delivered (the controller has information about θ because it knows when to expect a packet), we compute the state prediction based on this measurement $y(k-1) = x(k-1) + w(k-1)$; if the packet is lost, we propagate the previous prediction $\hat{x}(k-1)$. As there is no feedback on lost control packets (i.e., about ϕ) and thus a potential mismatch between the computed input $\hat{u}(k-1)$ and the actual $u(k-1)$, the controller can only use $\hat{u}(k-1)$ in the prediction.

Using $\hat{x}(k)$, the controller has an estimate of the current state of the system. However, it will take another time step for the currently computed control input to arrive at the physical system. For computing the next control input, we thus propagate the system another step,

$$\hat{u}(k+1) = F(A\hat{x}(k) + B\hat{u}(k)), \quad (5)$$

where F is as in the nominal design. The input $\hat{u}(k+1)$ is then transmitted over the wireless network.

The overall controller design requires only a few matrix multiplications per execution. This can be efficiently implemented on embedded devices, thus satisfying goal **G5**.

4.3 Stability Analysis

We now develop a stability proof for the closed-loop system given by the dynamic system of §4.1 and the proposed controller from §4.2. Because the model in §4.1 incorporates the physical process and the essential properties of the wireless embedded system, we will thus achieve goal **G4**.

While the process dynamics (2) are time invariant, the packet losses introduce time variation and randomness into the system dynamics. Therefore, we will leverage stability results for linear, stochastic, time-varying systems [11]. For simplicity, we will consider (2) without process and measurement noise ($v(k) = 0$ and $w(k) = 0$), and comment later on extensions. We first introduce required definitions and preliminary results, and then apply these to our problem.

Consider the system

$$z(k+1) = \tilde{A}(k)z(k) \quad (6)$$

with state $z(k) \in \mathbb{R}^n$ and $\tilde{A}(k) = \tilde{A}_0 + \sum_{i=1}^L \tilde{A}_i p_i(k)$, where $p_i(k)$ are i.i.d. random variables with mean $\mathbb{E}[p_i(k)] = 0$, variance $\text{Var}[p_i(k)] = \sigma_{p_i}^2$, and $\mathbb{E}[p_i(k)p_j(k)] = 0 \forall i, j$.

A common stability notion for stochastic systems like (6) is mean-square stability:

DEFINITION 1 ([11, p. 131]). *Let $Z(k) := \mathbb{E}[z(k)z^T(k)]$ denote the state correlation matrix. The system (6) is mean-square stable (MSS) if $\lim_{k \rightarrow \infty} Z(k) = 0$ for any initial $z(0)$.*

That is, a system is called MSS if the state correlation vanishes asymptotically for any initial state. MSS implies, for example, that $z(k) \rightarrow 0$ almost surely, [11, p. 131].

In control theory, linear matrix inequalities (LMIs) are often used as computational tools to check for system properties such as stability (see [11] for an introduction and details). For MSS, we shall employ the following LMI stability result:

LEMMA 1 ([11, p. 131]). *System (6) is MSS if, and only if, there exists a positive definite matrix $P > 0$ such that*

$$\tilde{A}_0^T P \tilde{A}_0 - P + \sum_{i=1}^L \sigma_{p_i}^2 \tilde{A}_i^T P \tilde{A}_i < 0. \quad (7)$$

We will now apply this result to the system and controller from §4.1 and §4.2. The closed-loop dynamics are given by

(2)–(5), which we rewrite as an augmented system

$$\underbrace{\begin{pmatrix} x(k+1) \\ \hat{x}(k+1) \\ u(k+1) \\ \hat{u}(k+1) \end{pmatrix}}_{z(k+1)} = \underbrace{\begin{pmatrix} A & 0 & B & 0 \\ \theta A & (1-\theta)A & 0 & B \\ 0 & 0 & (1-\phi)I & \phi I \\ 0 & FA & 0 & FB \end{pmatrix}}_{\tilde{A}(k)} \underbrace{\begin{pmatrix} x(k) \\ \hat{x}(k) \\ u(k) \\ \hat{u}(k) \end{pmatrix}}_{z(k)}. \quad (8)$$

The system has the form of (6); the transition matrix depends on θ and ϕ , and thus on time (omitted for simplicity). We can thus apply Lemma 1 to obtain our main stability result.

THEOREM 1. *The system (8) is MSS if, and only if, there exists a $P > 0$ such that (7) holds with*

$$\tilde{A}_0 = \begin{pmatrix} A & 0 & B & 0 \\ \mu_\theta A & (1-\mu_\theta)A & 0 & B \\ 0 & 0 & (1-\mu_\phi)I & \mu_\phi I \\ 0 & FA & 0 & FB \end{pmatrix}, \quad \tilde{A}_1 = \begin{pmatrix} 0 & 0 & 0 & 0 \\ -\mu_\theta A & \mu_\theta A & 0 & 0 \\ 0 & 0 & 0 & 0 \\ 0 & 0 & 0 & 0 \end{pmatrix},$$

$$\tilde{A}_2 = \begin{pmatrix} 0 & 0 & 0 & 0 \\ 0 & 0 & 0 & 0 \\ 0 & 0 & \mu_\phi I & -\mu_\phi I \\ 0 & 0 & 0 & 0 \end{pmatrix}, \quad \sigma_{p_1}^2 = 1/\mu_\theta - 1, \quad \sigma_{p_2}^2 = 1/\mu_\phi - 1.$$

PROOF. For clarity, we reintroduce time indices for θ and ϕ here. Following a similar approach as in [58], we transform $\theta(k)$ as $\theta(k) = \mu_\theta(1 - \delta_\theta(k))$ with the new binary random variable $\delta_\theta(k) \in \{1, 1 - 1/\mu_\theta\}$ with $\mathbb{P}[\delta_\theta(k) = 1] = 1 - \mu_\theta$ and $\mathbb{P}[\delta_\theta(k) = 1 - 1/\mu_\theta] = \mu_\theta$; and analogously for $\phi(k)$ and $\delta_\phi(k)$. We thus have that $\delta_\theta(k)$ is i.i.d. (because θ is i.i.d.) with $\mathbb{E}[\delta_\theta(k)] = 0$ and $\text{Var}[\delta_\theta(k)] = \sigma_{p_1}^2$, and similarly for $\delta_\phi(k)$. Employing this transformation, $\tilde{A}(k)$ in (8) is rewritten as $\tilde{A}(k) = \tilde{A}_0 + \sum_{i=1}^2 \tilde{A}_i p_i(k)$ with $p_1(k) = \delta_\theta(k)$, $p_2(k) = \delta_\phi(k)$, and \tilde{A}_i as stated above. Thus, all properties of (6) are satisfied, and Lemma 1 yields the result. \square

Using Theorem 1, we can analyze stability for any concrete physical system (2) (noise-free), a state-feedback controller F , and probabilities μ_θ and μ_ϕ . Searching for a $P > 0$ that satisfies the LMI (7) can be done using efficient numerical tools based on convex optimization (e.g., [24, 29, 41]). If such a P is found, we have the stability guarantee **(G4)**.

The stability analysis can be extended to account for process and measurement noise so that MSS then implies bounded $Z(k)$ (see [11, p. 138]). Moreover, other combinations of end-to-end delay T_D and update interval T_U are possible, including $T_D = nT_U$ ($n \in \mathbb{N}$). Also the ‘sensor to controller’ and ‘controller to actuator’ delays may be different.

4.4 Multi-agent Synchronization

In distributed or decentralized control architectures, different controllers have access to different measurements and inputs, and thus, in general, different information. This is the core reason for why such architectures are more challenging than centralized ones [31, 48]. Property **P3** of the wireless embedded system in §3 thus offers a key advantage over alternative networks. Because every agent in the network

has access to all information (except for rare packet loss), we can carry out a centralized design, but implement the resulting controllers in a distributed fashion. Such schemes have been used before for wired-bus networks (e.g., in [73]). Here, we present synchronization of multiple physical systems as an *example* of how distributed control tasks can easily be achieved with the proposed wireless control system **(G6)**.

The problem we consider is shown in Fig. 6 (right). We assume multiple physical processes as in (2), but with possibly different dynamics parameters (A_i , B_i , etc.). We understand synchronization in this setting as the goal of having the system state of different agents evolve together as close as possible. That is, we want to keep the error $x_i(k) - x_j(k)$ between the states of systems i and j small. Instead of synchronizing the whole state vector, also a subset of all states can be considered. Synchronization of multi-agent systems is a common problem and also occurs under the terms consensus or coordination [49]. For simplicity, we consider synchronization of two agents in the following, but the approach directly extends to more than two, as we show in §5.

We consider the architecture in Fig. 6, where each physical system is associated with a local controller that receives local observations directly, and observations from other agents over the network. We present an approach based on linear quadratic optimal control (LQR) [3] to design the synchronizing controllers. We choose the quadratic cost function

$$J = \lim_{K \rightarrow \infty} \mathbb{E} \left[\sum_{k=0}^{K-1} \sum_{i=1}^2 \left(x_i^T(k) Q_i x_i(k) + u_i^T(k) R_i u_i(k) \right) + (x_1(k) - x_2(k))^T Q_{\text{sync}} (x_1(k) - x_2(k)) \right] \quad (9)$$

which expresses our objective of keeping $x_1(k) - x_2(k)$ small (through the weight $Q_{\text{sync}} > 0$), next to usual penalties on states ($Q_i > 0$) and control inputs ($R_i > 0$). Using augmented state $\tilde{x}(k) = (x_1(k), x_2(k))^T$ and input $\tilde{u}(k) = (u_1(k), u_2(k))^T$, the term in the summation over k can be rewritten as

$$\tilde{x}^T(k) \begin{pmatrix} Q_1 + Q_{\text{sync}} & -Q_{\text{sync}} \\ -Q_{\text{sync}} & Q_2 + Q_{\text{sync}} \end{pmatrix} \tilde{x}(k) + \tilde{u}^T(k) \begin{pmatrix} R_1 & 0 \\ 0 & R_2 \end{pmatrix} \tilde{u}(k).$$

Thus, the problem is in standard LQR form and can be solved with standard tools [3]. The optimal stabilizing controller that minimizes (9) has the structure $u_1(k) = F_{11}x_1(k) + F_{12}x_2(k)$ and $u_2(k) = F_{21}x_1(k) + F_{22}x_2(k)$; that is, agent 1 ($u_1(k)$) requires state information from agent 2 ($x_2(k)$), and vice versa. Because of many-to-all communication, the wireless embedded system directly supports this (as well as any other possible) controller structure **(P3)**.¹

¹As the controller now runs on the node that is collocated with the physical process, local measurements and inputs are not sent over the wireless network, and the local sampling time can be shorter than T_U (measurements from other agents are still received over the network every T_U). While the analysis in §4.3 can be generalized to the synchronization setting, a formal

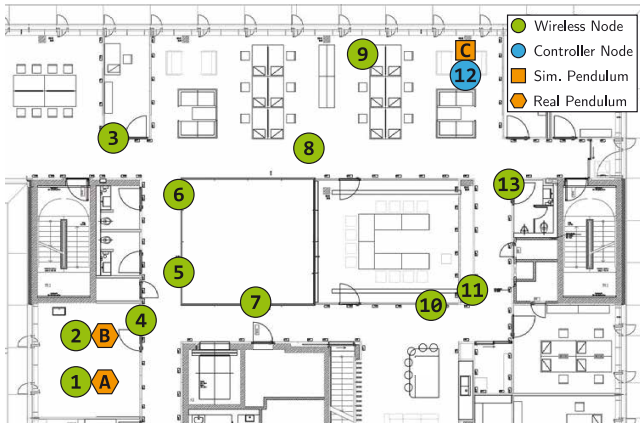


Figure 7: Testbed with nodes and pendulums. For multi-hop stabilization (§5.2), a controller running on node 12 stabilizes the inverted pendulums A and B. For multi-hop synchronization (§5.5), nodes 1, 2, and 12 stabilize the collocated pendulums while synchronizing the movement of the carts.

5 EXPERIMENTAL EVALUATION

In this section, we evaluate the proposed integrated design. Our goal is to answer the following questions:

- 1) Does our design enable fast closed-loop control over multi-hop low-power wireless networks?
- 2) What is the impact of delays and (bursty) message losses on control and network performance?
- 3) Is our system design flexible enough to support different control and coordination scenarios?

Before discussing our results in detail, we describe the testbed, physical system, and settings we use.

5.1 Methodology

Testbed. As shown in Fig. 7, our testbed consists of 13 DPP nodes and 2 physical systems spread out across an area of around 15 m x 20 m in an office building with all kinds of walls, from thin glass to reinforced concrete. Transmitting at 10 dBm, the nodes form a 3-hop network while being exposed to interference from other electronics and people’s activity. Two DPP nodes are connected to physical systems.

Physical system. We use *cart-pole systems*, also known as *pendulums*, which are widely used in control research [10]. As shown in Fig. 8, a cart-pole system consists of a cart that can move horizontally on a track and a pole attached to it via a revolute joint. The cart is equipped with a DC motor, which can be controlled by applying a certain voltage in order to influence the speed and the direction of the cart movements. Moving the cart exerts a force on the pole and thus allows to influence the pole angle θ . This way, the pole

stability proof is beyond the scope of this paper. In general, stability is less critical here because of shorter update intervals in the local feedback loop.

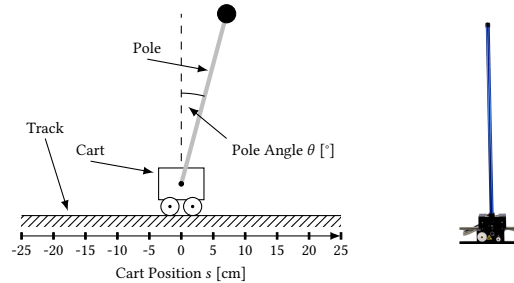


Figure 8: Schematic and photo of the cart-pole system. By controlling the force applied to the cart, the pole can be stabilized in the upright position around $\theta = 0^\circ$.

can be stabilized in an upright position (*i.e.*, $\theta = 0^\circ$), which is an inherently unstable equilibrium and called the *inverted pendulum*. The dynamics and time constants of the inverted pendulum are on the order of a few tens of milliseconds and representative of many real-world mechanical systems.

For small deviations from the equilibrium, the inverted pendulum can be well approximated by an LTI system as in (2a). The state $x(k)$ of the system consists of four variables. Two of them, the pole angle $\theta(k)$ and the cart position $s(k)$, can be measured with angle sensors. Their derivatives, the angular velocity $\dot{\theta}(k)$ and cart velocity $\dot{s}(k)$, can be estimated using, for example, finite differences and low-pass filtering. The voltage applied to the motor is the control input $u(k)$.

The cart-pole system is subject to a few constraints. Control inputs are capped at ± 10 V. The track for the cart has a usable length of ± 25 cm from the center (see Fig. 8). Surpassing these track limits immediately ends an experiment.

The AP of a co-located node reads out the angle sensors through an interconnect board equipped with quadrature decoders and crystals. The (control) input voltage is applied via a digital-to-analog converter coupled with an amplifier to enable a range of ± 10 V. Measurements and control inputs are low-pass filtered (*e.g.*, to prevent aliasing effects [27]).

Scenarios. We consider stabilization and synchronization as introduced in §4. For stabilization, we use two inverted pendulums connected to nodes 1 and 2, as shown in Fig. 7. A remote controller running on the AP of node 12 keeps the pole of both pendulums in an upright position. The remote stabilization scenario is relevant, for example, because it resembles practical situations in large-scale processes where sensing and actuation happen at different locations, and it allows us to show the limits of the proposed approach.

For synchronization, we replace the controller on node 12 with a simulated pendulum running on a collocated PC. The simulated pendulum is based on a model provided by the manufacturer [56]. As described in §4.4, each node attached to a pendulum runs a local controller for stabilization and shares its state information for synchronization with the

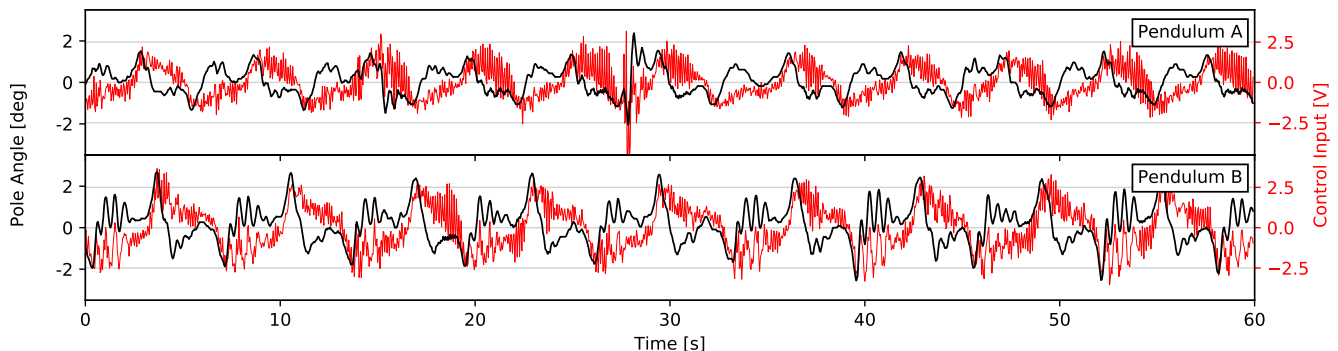


Figure 9: Pole angle and control input when stabilizing two inverted pendulums over multiple wireless hops. Both pendulums stabilize around a pole angle of 0° while applying roughly ± 2.5 V, which is only one quarter of the possible input voltage.

other two nodes. The objective is to synchronize the cart positions so that the three carts shall all move in concert.

Metrics. To judge control performance, we record pole angle, cart position, and control input. In addition, we measure radio duty cycle in software and log lost messages. At the beginning of each experiment, we manually move the poles in an upright position in the middle of the track; then the controller takes over. We repeat each experiment three times and present averages, distribution, etc. across all runs. Plots showing a metric over time are representative examples.

5.2 Multi-hop Stabilization

In our first experiment, we want to answer the main question of our work and investigate the feasibility of fast closed-loop control over multi-hop low-power wireless networks.

Finding: We can safely stabilize two inverted pendulums via a remotely located controller across multiple wireless hops.

Setup. We configure the wireless embedded system and the controller for an update interval of $T_U = 40$ ms ($T_D = 80$ ms). We design the controller as outlined in §4.2, and choose the feedback matrix F such that we get closed-loop eigenvalues at 0.8, 0.85, and 0.9 (twice). Using Theorem 1, we can prove stability for the overall system using $\mu_\theta = \mu_\phi = 0.999$ as per property **P2**. Thus, the theoretical analysis matches the experimental finding above. For predictions, controller design, and stability proof we use matrices A and B from [56].

Results. Fig. 9 shows the pole angle and the corresponding control input of each pendulum over time. Both pendulums exhibit periodic movement patterns, which differ slightly due to different friction and weight. The control input varies between -2.5 V and 2.5 V, using at most one quarter of the possible input voltage. We thus conclude that we can safely stabilize two inverted pendulums in the given setup with an update interval of 40 ms. No message was lost throughout the three runs, yielding an end-to-end reliability of 100 %.

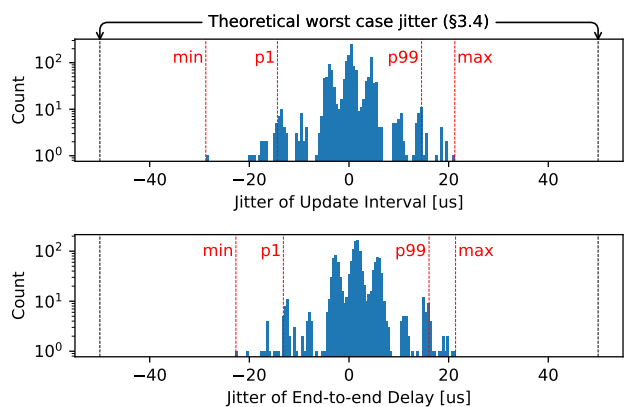


Figure 10: Jitter on update interval and end-to-end delay measured during the experiment shown in Fig. 9. We validate that the measured jitter is indeed smaller than the theoretical worst-case jitter we compute in §3.4.

Validation of jitter analysis. During the same experiment, we also measure T_U and T_D using a logic analyzer connected to GPIO pins of node 1. The pins are set when the state of the pendulum is captured and when the control input is applied. Fig. 10 plots the jitter on T_U and T_D . We see that the empirical results are well within the theoretical worst-case bounds, which validates our jitter analysis and assumptions in §4.

5.3 Impact of Update Interval and Delay

We take a closer look at the impact of different update intervals (and hence end-to-end delays) on control performance.

Finding: Larger update intervals decrease control performance, but enable energy savings on the communication side.

Setup. To minimize effects that we cannot control such as external interference, we use only node 1 connected to the pendulum while node 2 runs the controller. We use the controller from before, but adjust the feedback matrix F for each update interval to achieve similar closed-loop behavior.

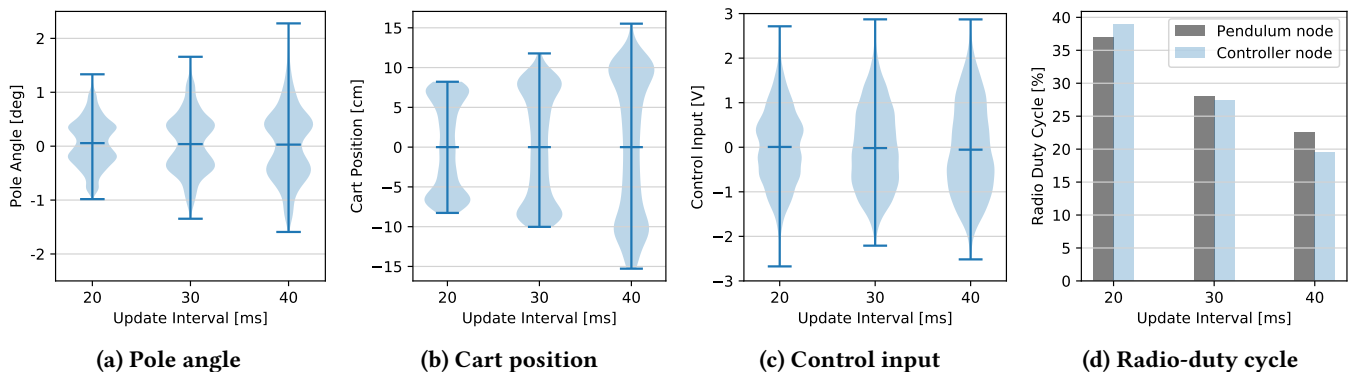


Figure 11: Distribution of control performance with minimum, maximum, and average highlighted in (a)–(c) and average radio duty cycle in (d) when remotely stabilizing a pendulum across one hop for different update intervals. A larger update interval leads to larger pole angles and more movement of the cart, while reducing the average radio duty cycle.

Results. Fig. 11 shows control performance and radio duty cycle for varying update intervals based on three 1-minute runs each. We see our system supports update intervals from 20 ms to 40 ms. A larger update interval leads to larger pole angles and more movement of the cart. This can be explained by looking at the control input. There is not much of a change for the extrema, but the distribution of the data changes. At a higher update interval, higher control inputs occur more often, leading to more movement of the cart. At the same time, doubling the update interval decreases the radio duty cycle of the two nodes by 39% and 50%, respectively.

5.4 Resilience to Message Loss

Next, we evaluate the impact of message losses, which are a well-known phenomenon in wireless networks [66].

Finding: *Our system can stabilize an inverted pendulum at an update interval of 20 ms despite 75% i.i.d. Bernoulli losses and in situations with bursts of 40 consecutively lost messages.*

Setup. We use again the controller and 2-node setup from before with a fixed update interval of 20 ms. To precisely control the message loss, we let both nodes intentionally drop messages in two different ways. In a first experiment, nodes independently drop a received message according to a Bernoulli process with given failure probability. In a second one, nodes drop a certain number of consecutive packets, leaving 10 s between bursts to let the pendulum recover.

Results. Fig. 12a–c shows results for varying i.i.d. Bernoulli message loss rates. Pole angle, control input, and total distance moved by the cart increase with rising message loss rate. Even at 85% message loss, our system is able to stabilize the pendulum most of the time. One reason why the pendulum can be stabilized despite such a high message loss rate is the short update interval. For example, losing 50% of the messages at an update interval of 20 ms essentially leads

to an average update interval of 40 ms, which is enough to stabilize the pendulum as shown in the previous experiment.

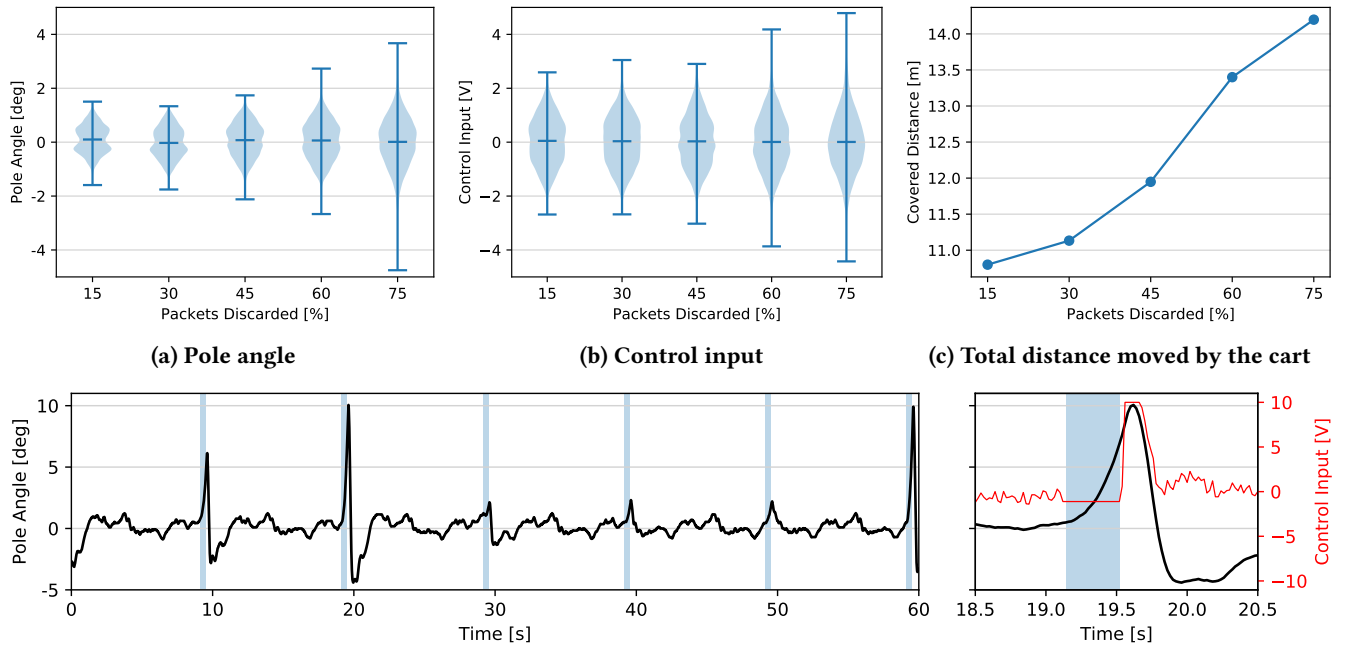
To study the impact of correlated message losses, we experiment with bursts between 10 and 40 consecutively lost messages. Fig. 12d shows the impact of burst losses on the pole angle for a burst length of 40. We always stabilize the pendulum up to a burst length of 30, and even 40 consecutive losses are tolerable most of the time as visible in Fig. 12d. The impact depends on the state of the pendulum. A burst happening while the pendulum is moving is much more critical than a burst during calm situations where only little actuation is needed. This can be seen, for example, by comparing the second with the third burst phase in Fig. 12d; the plot to the right zooms in on the second burst phase. The control input is close to 0 V during the burst phase. As soon as the burst begins, the pole angle diverges from the equilibrium at 0° due to the system’s unstable dynamics in the absence of feedback. Usually it takes the pendulum between 1 s and 2 s after the burst to get back into a normal operation regime.

5.5 Multi-hop Synchronization

To answer our last question and assess the suitability and flexibility of our system for distributed control over wireless, we set up a multi-hop synchronization experiment. The goal is to synchronize the cart positions of three pendulums. We follow the approach outlined in §4.4. Therefore, every pendulum requires the state of the other two pendulums.

Finding: *Three pendulum systems (two real, one simulated) can be synchronized reliably over a multi-hop wireless network.*

Setup. We perform three different experiments. In the first one, synchronization is disabled. This serves as a baseline for the second experiment in which synchronization is enabled. During a third experiment with synchronization enabled, we manually pull and hold one pendulum at a specific position to see how the other two pendulums react. We use identical



(d) Pole angle for bursts of 40 consecutive losses every 10 s (shaded areas). The plot to the right zooms in on the second burst.

Figure 12: Control performance when remotely stabilizing one pendulum over one hop under artificially injected message loss, for i.i.d. Bernoulli losses in (a)–(c) and for longer bursts of multiple consecutive losses in (d). Depending on the update interval, the pole can be stabilized despite significant and bursty message loss, albeit with reduced performance.

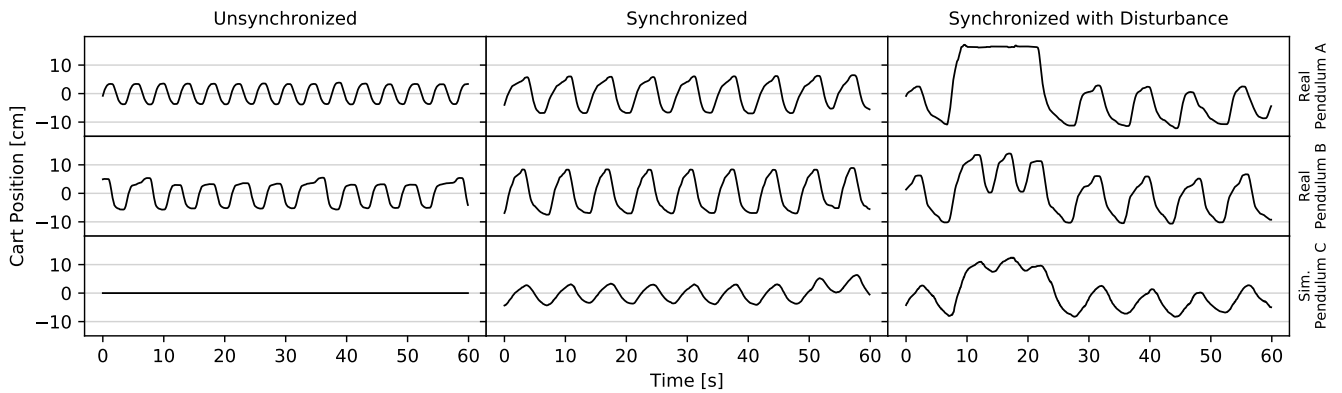


Figure 13: Cart position of three inverted pendulums over time (two real pendulums at the top, one simulated pendulum at the bottom), which are stabilized through local control at update intervals of 10 ms (real pendulums) and 20 ms (simulated pendulum), while the positions of the carts are simultaneously synchronized over a multi-hop low-power wireless network with an update interval of 50 ms (second and third column). With synchronization enabled, all three carts move in concert and even try to mimic the temporary disturbance of the topmost pendulum.

Q_i in (9) for all three pendulums, following a suggested LQR design in [56], and set $R_i = 0.2$. As we here care to synchronize the cart positions, we set the first diagonal entry of Q_{sync} to 10 and all others to 0. The local control for stabilization via the AP of nodes 1, 2, and 12 executes with an update interval of 10 ms for the real pendulums and 20 ms for the simulated

one, while the three nodes exchange state information every 50 ms over the multi-hop network for synchronization.

Results. The first column in Fig. 13 shows the cart positions without synchronization. The simulated pendulum perfectly stabilizes at 0, while the real pendulums vary slightly

around this equilibrium due to, for example, imperfect measurements. Despite the same controller implementation, the movement patterns of the real pendulums differ in frequency and amplitude because of small differences in their physics.

The second column shows the behavior when synchronization is enabled. We see that the frequencies and amplitudes of the cart movements are aligned, especially when looking at the simulated cart, which did not move in the first run.

During the third experiment, we manually hold the cart of pendulum A for 15 s at around 15 cm. The position of the fixed pendulum A affects the behavior of the other two, which move toward this position. However, as the controllers also need to stabilize the system, they do not fully reach the fixed position, but rather oscillate to balance the poles.

While we present experiments with three pendulum here, more pendulums can be supported at the expense of longer update intervals for state exchange over the network.

6 RELATED WORK

The control community has extensively studied design and stability analysis for different architectures, delay models, and message loss processes [47, 64, 74, 77, 82]. Recent surveys provide an overview of this large body of fundamental work [34, 81]. Toolboxes have been developed to evaluate control designs in simulation based on an abstract model of an imperfect network [8, 15]. Similarly, co-design based on an integration of control and real-time scheduling theory [13] and formal analysis of closed-loop properties using hybrid automata modeling physical, control, and network-induced timing aspects [28] have been proposed. We build on these foundations, but also validate our control design and analysis in a wireless testbed with real physical systems.

Turning to the sensor network, embedded, and real-time communities, we find related work on how to achieve real-time communication across distributed, unreliable, and dynamic networks of resource-constrained devices [69]. Early efforts based on asynchronous multi-hop routing provide soft guarantees on end-to-end message deadlines [33, 46]. Solutions from industry and academia have been proposed [16, 17, 54, 63] and analyzed [60, 61, 80], targeting real-time monitoring in static networks with a few sinks. Using a flooding-based approach, real-time communication in dynamic networks with any number of sinks has been demonstrated [85]. The problem of lifting real-time guarantees from the network to the application level is studied in [38], but the achievable end-to-end latencies on the order of seconds are too long for emerging closed-loop control applications [1]. We also build on Glossy [26], but show how to achieve end-to-end latencies in the tens of millisecond range with bounded jitter.

Co-design of control and routing based on WirelessHART has been studied in simulation [44, 53]. While [44] focuses

on the impact of the routing strategy on control performance, the work in [53] proposes to adapt the network protocol at runtime in response to changes in the state of the physical system. We use similar techniques to deal with message loss, but present an integrated design that allows for stability guarantees regardless of network dynamics, supports update intervals of tens of milliseconds, and works on real multi-hop networks. Perhaps more fundamentally, we show that well-known, simple control and coordination techniques can be straightforwardly applied to a real wireless system design thanks to the properties **P1–P4**. Routing-based approaches, on the other hand, are less flexible (in terms of control scenarios and the required traffic patterns) and less robust (to dynamic changes in the network topology), require more complex techniques on the control side (e.g., because packet losses are highly correlated), and thus may not allow for formal stability guarantees that also hold in the real world.

Practical efforts on control over wireless fall in two categories. First, multi-hop solutions based on low-power 802.15.4 devices exist for physical systems with *slow dynamics* achieving update intervals on the order of seconds, such as adaptive lighting in road tunnels [12] and power management in data centers [59]. Second, solutions for physical systems with *fast dynamics* providing update intervals below 100 ms are exclusively based on single-hop networks of 802.11 [55, 79], Bluetooth [23], or 802.15.4 [8, 52] devices. Instead, we demonstrate fast closed-loop control and coordination with guaranteed stability over multi-hop 802.15.4 networks.

7 CONCLUSIONS

We have presented an end-to-end low-power wireless CPS design that demonstrates for the first time closed-loop control over multiple hops with update intervals from 20 ms to 50 ms. The design allows for stability guarantees and supports coordination tasks. Experiments on a testbed with multiple physical systems reveal the robustness and performance trade-offs of our approach. Thus, by demonstrating how to close feedback loops quickly and reliably over long distances in the face of network dynamics, this paper represents an important stepping stone towards realizing the CPS vision.

Acknowledgments. We thank Harsoveet Singh and Felix Grimminger for their help with the experimental setup. This work was supported in part by the German Research Foundation (DFG) within the Cluster of Excellence CFAED and SPP 1914 (grants ZI 1635/1-1 and TR 1433/1-1), the Cyber Valley Initiative, and the Max Planck Society.

REFERENCES

- [1] J. Akerberg, M. Gidlund, and M. Bjorkman. 2011. Future research challenges in wireless sensor and actuator networks targeting industrial automation. In *IEEE International Conference on Industrial Informatics (INDIN 2016)*.

- [2] A. Alam, B. Besselink, V. Turri, J. Martensson, and K. H. Johansson. 2015. Heavy-duty vehicle platooning for sustainable freight transportation: A cooperative method to enhance safety and efficiency. *IEEE Control Systems Magazine* 35, 6 (2015).
- [3] B. D. O. Anderson and J. B. Moore. 2007. *Optimal Control: Linear Quadratic Methods*. Dover Publications.
- [4] J. Araujo, M. Mazo, A. Anta, P. Tabuada, and K. H. Johansson. 2014. System architectures, protocols and algorithms for aperiodic wireless control systems. *IEEE Trans. on Industrial Informatics* 10, 1 (2014).
- [5] K. J. Åström and B. Wittenmark. 1996. *Computer-Controlled Systems: Theory and Design*. Prentice Hall.
- [6] K. J. Åström and B. Wittenmark. 2008. *Feedback Systems: An Introduction for Scientists and Engineers*. Princeton University Press.
- [7] J. Baillieul and P. J. Antsaklis. 2007. Control and Communication Challenges in Networked Real-Time Systems. *Proc. IEEE* 95, 1 (2007).
- [8] N. W. Bauer, S. J. Van Loon, N. Van De Wouw, and W. P. Heemels. 2014. Exploring the boundaries of robust stability under uncertain communication: An NCS toolbox applied to a wireless control setup. *IEEE Control Systems Magazine* 34, 4 (2014).
- [9] B. Besselink, V. Turri, S. H. Van De Hoef, K. Y. Liang, A. Alam, J. Martensson, and K. H. Johansson. 2016. Cyber-Physical Control of Road Freight Transport. *Proc. IEEE* 104, 5 (2016).
- [10] O. Boubaker. 2012. The inverted pendulum: A fundamental benchmark in control theory and robotics. In *International Conference on Education and e-Learning Innovations (ICEELI 2012)*.
- [11] S. Boyd, L. E. Ghaoui, E. Feron, and V. Balakrishnan. 1994. *Linear Matrix Inequalities in System & Control Theory*. Society for Industrial & Applied Mathematics.
- [12] M. Ceriotti, M. Corra, L. D’Orazio, R. Doriguzzi, D. Facchin, S. T. Guna, G. P. Jesi, R. L. Cigno, L. Mottola, A. L. Murphy, M. Pescalli, G. P. Picco, D. Pregolato, and C. Torghelle. 2011. Is there light at the ends of the tunnel? Wireless sensor networks for adaptive lighting in road tunnels. In *ACM/IEEE International Conference on Information Processing in Sensor Networks (IPSN 2011)*.
- [13] A. Cervin. 2003. *Integrated Control and Real-Time Scheduling*. Ph.D. Dissertation.
- [14] A. Cervin, J. Eker, B. Bernhardsson, and K.-E. Årzén. 2002. Feedback-Feedforward Scheduling of Control Tasks. *Real-Time Systems* 23, 1/2 (2002).
- [15] A. Cervin, D. Henriksson, B. Lincoln, J. Eker, and K.-E. Årzén. 2003. How Does Control Timing Affect Performance? Analysis and Simulation of Timing Using Jitterbug and TrueTime. *IEEE Control Systems Magazine* (2003).
- [16] O. Chipara, C. Lu, and G.-C. Roman. 2007. Real-Time Query Scheduling for Wireless Sensor Networks. In *IEEE International Real-Time Systems Symposium (RTSS 2007)*.
- [17] O. Chipara, C. Wu, C. Lu, and W. Griswold. 2011. Interference-aware real-time flow scheduling for wireless sensor networks. In *Euromicro Conference on Real-Time Systems (ECRTS 2011)*.
- [18] P. Corke, T. Wark, R. Jurdak, W. Hu, P. Valencia, and D. Moore. 2010. Environmental wireless sensor networks. *Proc. IEEE* 98, 11 (2010).
- [19] N. Correll, P. Dutta, R. Han, and K. Pister. 2017. New Directions: Wireless Robotic Materials. In *ACM Conference on Embedded Network Sensor Systems (SenSys 2017)*.
- [20] S. Dawson-Haggerty, A. Krioukov, J. Taneja, S. Karandikar, G. Fierro, N. Kitaev, and D. Culler. 2013. BOSS: building operating system services. In *USENIX Conference on Networked Systems Design and Implementation (NSDI 2013)*.
- [21] P. Derler, E. A. Lee, and A. Sangiovanni Vincentelli. 2012. Modeling cyber-physical systems. *Proc. IEEE* 100, 1 (2012).
- [22] S. Duquenooy, B. Al Nahas, O. Landsiedel, and T. Watteyne. 2015. Orchestra: Robust Mesh Networks Through Autonomously Scheduled TSCH. In *ACM Conf. on Embedded Networked Sensor Systems (SenSys 2015)*.
- [23] J. Eker, A. Cervin, and A. Horjel. 2001. Distributed Wireless Control Using Bluetooth. In *IFAC Conference on New Technologies for Computer Control*.
- [24] L. El Ghaoui, F. Delebecque, and R. Nikoukhan. 1995. *LMI TOOL: A user-friendly Interface for LMI Optimization*. Technical Report.
- [25] F. Ferrari, M. Zimmerling, L. Mottola, and L. Thiele. 2012. Low-power wireless bus. In *ACM Conference on Embedded Network Sensor Systems (SenSys 2012)*.
- [26] F. Ferrari, M. Zimmerling, L. Thiele, and O. Saukh. 2011. Efficient network flooding and time synchronization with Glossy. In *ACM/IEEE International Conference on Information Processing in Sensor Networks (IPSN 2011)*.
- [27] G. F. Franklin, J. D. Powell, and A. Emami-Naeini. 1994. *Feedback Control of Dynamic Systems*. Addison-Wesley.
- [28] G. Frehse, A. Hamann, S. Quinton, and M. Woehrle. 2014. Formal analysis of timing effects on closed-loop properties of control software. In *IEEE Real-Time Systems Symposium (RTSS 2014)*.
- [29] P. Gahinet, A. Nemirovskii, A. J. Laub, and M. Chilali. 1994. The LMI control toolbox. In *IEEE Conference on Decision and Control*.
- [30] O. Gnawali, R. Fonseca, K. Jamieson, D. Moss, and P. Levis. 2009. Collection tree protocol. In *ACM Conference on Embedded Networked Sensor Systems (SenSys 2009)*.
- [31] P. Grover. 2014. Information Structures, the Witsenhausen Counterexample, and Communicating Using Actions. *Encyclopedia of Systems and Control* (2014).
- [32] S. Hayat, E. Yanmaz, and R. Muzaffar. 2016. Survey on Unmanned Aerial Vehicle Networks for Civil Applications: A Communications Viewpoint. *IEEE Communications Surveys and Tutorials* 18, 4 (2016).
- [33] T. He, J. A. Stankovic, C. Lu, and T. Abdelzaher. 2003. SPEED: a stateless protocol for real-time communication in sensor networks. In *IEEE International Conference on Distributed Computing Systems (ICDCS 2003)*.
- [34] J. Hespanha, P. Naghshtabrizi, and Y. Xu. 2007. A Survey of Recent Results in Networked Control Systems. *Proc. IEEE* 95, 1 (2007).
- [35] J. P. Hespanha. 2009. *Linear Systems Theory*. Princeton University Press.
- [36] T. Istomin, A. L. Murphy, G. P. Picco, and U. Raza. 2016. Data Prediction + Synchronous Transmissions = Ultra-low Power Wireless Sensor Networks. In *ACM Conference on Embedded Network Sensor Systems (SenSys 2016)*.
- [37] R. Jacob, L. Zhang, M. Zimmerling, J. Beutel, S. Chakraborty, and L. Thiele. 2017. *TTW: A Time-Triggered-Wireless Design for CPS*. Technical Report. <http://arxiv.org/abs/1711.05581>
- [38] R. Jacob, M. Zimmerling, P. Huang, J. Beutel, and L. Thiele. 2016. End-to-End Real-Time Guarantees in Wireless Cyber-Physical Systems. In *IEEE Real-Time Systems Symposium (RTSS 2016)*.
- [39] J. Karschau, M. Zimmerling, and B. M. Friedrich. 2018. Renormalization group theory for percolation in time-varying networks. *Scientific Reports* (2018). <https://arxiv.org/pdf/1708.05704.pdf> In press.
- [40] H. Kopetz and G. Bauer. 2003. The time-triggered architecture. *Proc. IEEE* 91, 1 (2003).
- [41] Y. Labit, D. Peaucelle, and D. Henrion. 2002. SEDUMI INTERFACE 1.0.2: A tool for solving LMI problems with SEDUMI. In *IEEE International Symposium on Computer Aided Control System Design (CACSD 2002)*.
- [42] C. Lenzen, P. Sommer, and R. Wattenhofer. 2015. PulseSync: An Efficient and Scalable Clock Synchronization Protocol. *IEEE/ACM Transactions on Networking* 23, 3 (2015).
- [43] A. Lessard and M. Gerla. 1988. Wireless communications in the automated factory environment. *IEEE Network* 2, 3 (1988).

- [44] B. Li, Y. Ma, T. Westebroek, C. Wu, H. Gonzalez, and C. Lu. 2016. Wireless Routing and Control: A Cyber-Physical Case Study. In *ACM/IEEE International Conference on Cyber-Physical Systems (ICCPS 2016)*.
- [45] L. Li, D. Wen, and D. Yao. 2014. A survey of traffic control with vehicular communications. *IEEE Transactions on Intelligent Transportation Systems* 15, 1 (2014).
- [46] C. Lu, B. M. Blum, T. F. Abdelzaher, J. A. Stankovic, and T. He. 2002. RAP: A Real-Time Communication Architecture for Large-Scale Wireless Sensor Networks. In *IEEE Real-Time and Embedded Technology and Applications Symposium (RTAS 2002)*.
- [47] R. Luck and A. Ray. 1990. An observer-based compensator for distributed delays. *Automatica* 26, 5 (1990).
- [48] J. Lunze. 1992. *Feedback control of large scale systems*. Prentice-Hall.
- [49] J. Lunze. 2012. Synchronization of heterogeneous agents. *IEEE Trans. Automat. Control* 57, 11 (2012).
- [50] J. Lunze and L. Grüne. 2014. Introduction to Networked Control Systems. In *Control Theory of Digitally Networked Dynamic Systems*. Springer, Heidelberg.
- [51] M. Luvisotto, Z. Pang, and D. Dzung. 2017. Ultra High Performance Wireless Control for Critical Applications: Challenges and Directions. *IEEE Transactions on Industrial Informatics* 13, 3 (2017).
- [52] J. P. Lynch, Y. Wang, R. A. Swartz, K. C. Lu, and C. H. Loh. 2007. Implementation of a closed-loop structural control system using wireless sensor networks. *Structural Control and Health Monitoring* (2007).
- [53] Y. Ma, D. Gunatilaka, B. Li, H. Gonzalez, and C. Lu. 2017. *Holistic Cyber-Physical Management for Dependable Wireless Control Systems*. Technical Report. <http://arxiv.org/abs/1705.01862>
- [54] T. O'donovan, W.-B. Pöttner, U. Roedig, J. S. Silva, R. Silva, C. J. Sreenan, V. Vassiliou, T. Voigt, L. Wolf, Z. Zinonos, J. Brown, F. Büsching, A. Cardoso, J. Cecilio, J. D. Ó, P. Furtado, P. Gil, and A. Jugel. 2013. The GINSENG system for wireless monitoring and control. *ACM Transactions on Sensor Networks* 10, 1 (2013).
- [55] N. J. Ploplys, P. A. Kawka, and A. G. Alleyne. 2004. Closed-loop control over wireless networks. *IEEE Control Systems Magazine* 24, 3 (2004).
- [56] Quanser Inc. 2012. IP02 - Self-Erecting Single Inverted Pendulum (SESIP) - Linear Experiment #6: PV and LQR Control - Instructor Manual.
- [57] R. R. Rajkumar, I. Lee, L. Sha, and J. Stankovic. 2010. Cyber-Physical Systems: The Next Computing Revolution. In *ACM Design Automation Conference (DAC 2010)*.
- [58] M. Rich and N. Elia. 2015. Optimal mean-square performance for MIMO networked systems. In *American Control Conference (ACC 2015)*.
- [59] A. Saifullah, S. Sankar, J. Liu, C. Lu, R. Chandra, and B. Priyantha. 2014. CapNet: A real-time wireless management network for data center power capping. In *IEEE Real-Time Systems Symp. (RTSS 2014)*.
- [60] A. Saifullah, Y. Xu, C. Lu, and Y. Chen. 2010. Real-time scheduling for WirelessHART networks. In *IEEE Real-Time Systems Symposium (RTSS 2010)*.
- [61] A. Saifullah, Y. Xu, C. Lu, and Y. Chen. 2011. End-to-end delay analysis for fixed priority scheduling in WirelessHART networks. In *IEEE Real-Time and Embedded Technology and Applications Symp. (RTAS 2011)*.
- [62] C. B. Schindler, T. Watteyne, X. Vilajosana, and K. S. Pister. 2017. Implementation and characterization of a multi-hop 6TiSCH network for experimental feedback control of an inverted pendulum. In *International Symposium on Modeling and Optimization in Mobile, Ad Hoc, and Wireless Networks (WiOpt 2017)*.
- [63] S. M. Shahriar Nirjon, J. A. Stankovic, and K. Whitehouse. 2010. IAA: Interference aware anticipatory algorithm for scheduling and routing periodic real-time streams in wireless sensor networks. In *IEEE International Conference on Networked Sensing Systems (INSS 2010)*.
- [64] B. Sinopoli, L. Schenato, M. Franceschetti, K. Poolla, M. I. Jordan, and S. S. Sastry. 2004. Kalman filtering with intermittent observations. *IEEE Trans. on Automatic Control* 49, 9 (2004).
- [65] J. Skaf and S. Boyd. 2009. Analysis and Synthesis of State-Feedback Controllers With Timing Jitter. *IEEE Trans. on Automatic Control* 54, 3 (2009).
- [66] K. Srinivasan, P. Dutta, A. Tavakoli, and P. Levis. 2010. An empirical study of low-power wireless. *ACM Trans. on Sensor Networks* 6, 2 (2010).
- [67] K. Srinivasan, M. a. Kazandjieva, S. Agarwal, and P. Levis. 2008. The β -factor: Measuring Wireless Link Burstiness. In *ACM Conference on Embedded Network Sensor Systems (SenSys 2008)*.
- [68] J. A. Stankovic. 2016. Research Directions for Cyber Physical Systems in Wireless and Mobile Healthcare. *ACM Transactions on Cyber-Physical Systems* 1, 1 (2016).
- [69] J. A. Stankovic, T. F. Abdelzaher, C. Lu, L. Sha, and J. C. Hou. 2003. Real-time communication and coordination in embedded sensor networks. *Proc. IEEE* 91, 7 (2003).
- [70] F. Sutton, M. Zimmerling, R. Da Forno, R. Lim, T. Gsell, G. Giannopoulou, F. Ferrari, J. Beutel, and L. Thiele. 2015. Bolt: A Stateful Processor Interconnect. In *ACM Conference on Embedded Networked Sensor Systems (SenSys 2015)*.
- [71] J.-P. Thomesse. 2005. Fieldbus Technology in Industrial Automation. *Proc. IEEE* 93, 6 (2005).
- [72] P. Thubert. 2017. *An Architecture for IPv6 over the TSCH mode of IEEE 802.15.4*. Technical Report. <http://www.ietf.org/internet-drafts/draft-ietf-6tisch-architecture-13.txt>
- [73] S. Trimpe and R. D'Andrea. 2012. The balancing cube: A dynamic sculpture as test bed for distributed estimation and control. *IEEE Control Systems Magazine* 32, 6 (2012).
- [74] G. C. Walsh, H. Ye, and L. G. Bushnell. 2002. Stability analysis of networked control systems. *IEEE Transactions on Control Systems Technology* 10, 3 (2002).
- [75] T. Watteyne, V. Handziski, X. Vilajosana, S. Duquennoy, O. Hahn, E. Baccelli, and A. Wolisz. 2016. Industrial Wireless IP-Based Cyber-Physical Systems. *Proc. IEEE* 104, 5 (2016).
- [76] B. Wittenmark, J. Nilsson, and M. Törngren. 1995. Timing problems in real-time control systems. In *American Control Conference (ACC 1995)*.
- [77] J. Xiong and J. Lam. 2007. Stabilization of linear systems over networks with bounded packet loss. *Automatica* 43, 1 (2007).
- [78] T. Yang, H. Yu, M. Fei, and L. Li. 2005. Networked control systems: a historical review and current research topics. *Measurement & Control* 38, 1 (2005).
- [79] H. Ye, G. C. Walsh, and L. G. Bushnell. 2001. Real-Time Mixed-Traffic Wireless Networks. *IEEE Trans. on Industrial Electronics* 48, 5 (2001).
- [80] H. Zhang, P. Soldati, and M. Johansson. 2009. Optimal link scheduling and channel assignment for convergecast in linear WirelessHART networks. In *International Symposium on Modeling and Optimization in Mobile, Ad Hoc, and Wireless Networks (WiOpt 2009)*.
- [81] L. Zhang, H. Gao, and O. Kaynak. 2013. Network-induced constraints in networked control systems - A survey. *IEEE Transactions on Industrial Informatics* 9, 1 (2013).
- [82] W. Zhang, M. S. Branicky, and S. M. Phillips. 2001. Stability of networked control systems. *IEEE Control Systems Magazine* 21, 1 (2001).
- [83] G.-Y. Zhu and M. A. Henson. 2002. Model Predictive Control of Interconnected Linear and Nonlinear Processes. *Industrial & Engineering Chemistry Research* 41, 4 (2002).
- [84] M. Zimmerling, F. Ferrari, L. Mottola, and L. Thiele. 2013. On modeling low-power wireless protocols based on synchronous packet transmissions. In *IEEE Int. Symposium on Modeling, Analysis & Simulation of Computer and Telecommunication Systems (MASCOOTS 2013)*.
- [85] M. Zimmerling, L. Mottola, P. Kumar, F. Ferrari, and L. Thiele. 2017. Adaptive Real-Time Communication for Wireless Cyber-Physical Systems. *ACM Transactions on Cyber-Physical Systems* 1, 2 (2017).